

Article

Wind Environment Simulation and Optimisation Strategies for Block Spatial Forms in Cold Low Mountainous Areas—A Case Study of Changchun, China

Hongyu Zhao ¹, Xue Jiang ^{1,*}, Yujie Cao ², Haina Zhang ¹, Shinan Zhen ¹, Runze Jia ¹ and Shichao Zhang ¹

- ¹ School of Architecture and Planning, Jilin Jianzhu University, Changchun 130118, China; zhaohongyu@jlju.edu.cn (H.Z.); zhanghaina@student.jlju.edu.cn (H.Z.); zhenshinan@student.jlju.edu.cn (S.Z.); jiarunze@student.jlju.edu.cn (R.J.); zhangshichao@student.jlju.edu.cn (S.Z.)
- ² Shanghai Tongji Urban Planning Design Research Institute, Shanghai 200092, China; caoyujie@student.jlju.edu.cn
- * Correspondence: jiangxue@jlju.edu.cn; Tel.: +86-130-7432-1409

Abstract: Low mountainous areas provide high-quality ecological environments, offering a high urban development value globally. However, cold low mountainous areas are greatly affected by wind environments. Therefore, this study investigates a simulated block wind environment in a typical city in a cold low mountainous area. As opposed to previous work, we put forward the block spatial modes quantitatively for cold low mountainous areas. Computational fluid dynamics (CFD) technology is used to simulate the wind environment of building blocks, including point-type high-rise buildings and row-type multi-story buildings. We propose a new targeted wind environment measurement system developed using PHOENICS 2018 and a spatial combination model using urban information sensing for sustainable development. By comparing the average wind speed (W_{AS}) and calm wind area ratio (S_{CA}) under different simulation conditions, we were able to find that when the building form, slope direction, and slope were constant, W_{AS} was inversely proportional to S_{CA} , following the order of south slope > west slope > southwest slope > southeast slope. Second, proper selection of 1:2 and 1:3 ratios for point-type high-rise buildings (HPT) can provide good ventilation for cold low mountainous areas. In addition, continuous high-rise buildings should be avoided. These strategies have been applied in practice in the spatial design of the Lianhuashan tourist resort in Changchun. Possible optimization strategies for planners and governments could include promoting pedestrian spatial environments in these special areas. Moreover, this research is significant for the collection and mining of data-based wind information in cold low mountainous areas, thereby providing scientific quantitative evaluation methods and spatial organisation optimisation guidelines.



Citation: Zhao, H.; Jiang, X.; Cao, Y.; Zhang, H.; Zhen, S.; Jia, R.; Zhang, S. Wind Environment Simulation and Optimisation Strategies for Block Spatial Forms in Cold Low Mountainous Areas—A Case Study of Changchun, China. *Sustainability* **2022**, *14*, 6643. <https://doi.org/10.3390/su14116643>

Academic Editors: Xuan Song and Xiaodan Shi

Received: 24 April 2022

Accepted: 24 May 2022

Published: 28 May 2022

Publisher's Note: MDPI stays neutral with regard to jurisdictional claims in published maps and institutional affiliations.



Copyright: © 2022 by the authors. Licensee MDPI, Basel, Switzerland. This article is an open access article distributed under the terms and conditions of the Creative Commons Attribution (CC BY) license (<https://creativecommons.org/licenses/by/4.0/>).

Keywords: urban design; wind environment; thermal comfort; low mountainous areas; cold regions; spatial form

1. Introduction

Low mountainous areas are attracting increasing attention as important ecological areas, with relatively high population densities in many cities [1–3]. Such areas are not strictly a geographical unit, nor do they constitute a geomorphological type. Rather, a low mountainous area refers to the transitional area from high mountains to plains, including terrain features such as low elevation mountains, hills, terraced tablelands, and eroded gullies [2]. With rapid urbanisation and population growth after the Second World War, suitable flat land resources for construction have become increasingly scarce [3], resulting in increased urban construction activity in low mountainous areas in order to provide residential dwellings and recreation spaces for citizens. The altitude of low mountainous areas is typically in the 100–300 m range [1–3], with characteristic hilly terrain.

Furthermore, urban spatial organisation has a significant impact on regional liveability [4–6]. The wind environment of the block spatial form is a key topic in built environment research considering the comfort of outdoor spaces in low mountainous areas [1,7]. Moreover, the unique topographic characteristics of low mountainous areas have led to distinctive wind environments influenced by several factors, including velocity, direction, and turbulence [1,8].

Wind environment simulations of low mountainous areas have significant impacts on urban wind environmental improvement research [9,10]. Most recent studies on low mountainous areas have shown that wind environment simulations are affected by factors such as building style and topography. Other factors include the building packing density, which strongly affects city breathability within the urban canopy layer [11,12]. In many low mountainous areas, a comprehensive wind environment assessment is required to obtain a building permit from the city authority [13]. For example, technical guidelines prescribed by the Air Ventilation Assessment Technical Circular (AVA TC 2003) published in Hong Kong require wind tunnel experiments or computational fluid dynamics (CFD) simulations to be conducted for any land development procedure in order to ensure wind environment comfort at a pedestrian height [13–15]. However, due to the specificity of the simulation environment, a uniform standard for the construction of its spatial forms has not yet been adopted.

The research and simulation methods of urban spatial wind environments are quite sophisticated and include field tests, wind tunnel tests, and computer numerical simulations [15–17]. As the most widely used method in wind environment simulations, CFD is being increasingly applied to predict the wind environment around actual high-rise buildings, including the flow field around high-rise buildings and different types of building complexes in actual urban areas, [18,19], which presents clear advantages in urban microclimate research [20–22]. CFD analysis results in strong wind regions, showing a prediction accuracy within 10% for the standard $k-\epsilon$ model and better accuracy for the modified $k-\epsilon$ models [23]. Other research results have found that LES with a dynamic subgrid-scale model can provide satisfactory predictions of mean and dynamic wind loads on tall buildings, and has the additional advantage of providing rapid solutions. [24,25]. Such work requires a number of calculation cases, such as multiple wind directions, situations before and after construction of a proposed building, and measures after construction, and time for evaluation is limited in the practical design stages [23,26]. At the residential scale, it has been used to optimise the street design and to determine the location of air quality monitoring points by simulating the ventilation of residential streets bounded by different forms of buildings [27]. While the effects of urban morphology on outdoor ventilation, wind speed, and direction have been proven by multiple approaches, the versatility and high fidelity of CFD has enabled the quantitative assessment of outdoor ventilation design for generic configurations with parallel streets of equal and unequal widths [28].

However, previous wind environment simulations have mainly been conducted for Shenzhen, Macao, and other cities in South China. There is limited relevant research for cold cities, especially those in cold low mountainous areas [28,29]. The results of wind environment simulation analyses must be integrated into the construction of spatial forms in cold low mountainous areas. Here, we adopt CFD technology for the cold shallow mountainous area of Changchun, China, with its typical climate and terrain conditions, thereby addressing a gap in the literature. In terms of novelty, compared with previous works we put forward the block spatial modes quantitatively for cold shallow hilly areas. By comparing the average wind speed (W_{AS}) and calm wind area ratio (S_{CA}) under different simulation conditions, spatial optimization strategies for cold shallow mountainous areas can be proposed.

A notable example of a densely-populated cold low mountainous area is the Changbai Mountains region, where the climate notably affects northeast China, South Korea, North Korea, and the Russian far east. Nearly 30% of the land across the countries and provinces in the region is designated as special cold and low mountainous areas, with most of these

areas being densely populated [5,6]. As an example of a government administrative region at the large-province scale, Jilin Province in China has a population of more than 27 million people who are affected by this mountainous area. The capital city of Changchun has the highest population density in the province as well as a low-temperature climate that persists for more than 50% of the year, which leads to objectively poor thermal comfort in winter. Moreover, China has a vast amount of territory with a severe cold climate. Located in the southeast of Eurasia, it is often affected by cold air from Siberia during winter. Compared with other countries at the same latitude, the winter temperature of cold cities in China is much lower, with an average temperature below $-18\text{ }^{\circ}\text{C}$ in January [30]. Therefore, in this research Changchun was taken as a case study on wind environment simulation and optimisation strategies for block spatial forms in cold low mountainous areas.

In this study, we propose a new targeted wind environment measurement system using PHOENICS 2018 and a spatial combination model comparing the average wind speed and calm wind area ratio under different simulation conditions using urban information sensing for sustainable development. PHOENICS 2018 was used to extract the typical block spatial forms and process the CFD simulation progress, with automatic computational grid settings for improved accuracy and visualisation capabilities. The optimal spatial organisation in low mountainous areas was explored by inputting the regional wind direction and meteorological conditions and then applying the results to specific regional cases, which is an important aspect of sensing urban environmental changes. The effects of regional parameters such as wind pressure, wind speed, and comfort were simulated. Furthermore, PHOENICS is compatible with mainstream urban design software (such as AutoCAD, SketchUp, and 3ds Max), enabling easy interconvertibility between models in this study.

Due to the unique climate and geomorphic conditions of Changchun, China, the construction of the urban wind environment plays a key role in urban design. Starting with the most important elements of the wind environment, the simulation and optimisation path of block spatial forms are explored in this study to guide the construction and development of liveable cold city environments. From the perspective of wind environment simulations, the block organisation mode of Changchun, as a typical cold low mountainous area, may provide a point of reference for many countries and regions in similar areas. Optimization strategies are provided in order to promote pedestrian spatial environment planning for governments in these special areas, where the collection and mining of data-based wind information in these special areas can be helpful.

2. Data and Methods

2.1. Research Data

2.1.1. Meteorological Data

The basic wind data for Changchun were obtained from the Chinese Meteorological Administration and the Changchun City Meteorological Service. Parameters included the average wind speed and prevailing wind direction. For cold low mountainous areas, the parameters directly affecting the wind environment are the wind direction and wind speed [31,32]. The wind speed data used in the model were extracted from meteorological data sampled between 2011 and 2021, based on a total of 120 records. Furthermore, the prevailing wind direction was west–southwest throughout the year, whereas the overall wind speed was typically below 5.5 m/s.

2.1.2. Geographic Information Data

The acquisition of slope and aspect data is the premise of wind environment analysis in block spaces. Based on global positioning system (GPS) control points and field excursions, the average slope of the low mountainous area in Changchun was 5° . AutoCAD and SketchUp software were used to simulate the slope in the terrain. In the actual case analysis, remote sensing images were obtained from a multispectral unmanned aerial vehicle and

these were employed to extract slope data using a geographical information system (GIS) toolbox. The terrain data were imported into PHOENICS 2018 software for simulation analysis.

2.2. Research Method

2.2.1. Research Outline

First, the spatial forms of the low mountainous areas in Changchun were summarised based on their suitability for the wind environment and were divided into high-rise buildings of the point-type (HPT) and multi-story buildings of the row-type (MRT). Next, the wind environment of the corresponding spatial forms was calculated and simulated using the PHOENICS model. The wind environment was simulated at different altitudes under different modes by controlling the variables and the results were compared. On this basis, the data were processed using the MATLAB platform. After the analysis of the experimental results, an optimisation strategy was proposed based on the wind environment in order to guide revision of the urban design scheme. The research path is shown in Figure 1; the specific steps include the classification of the spatial form and the construction of the simulation model.

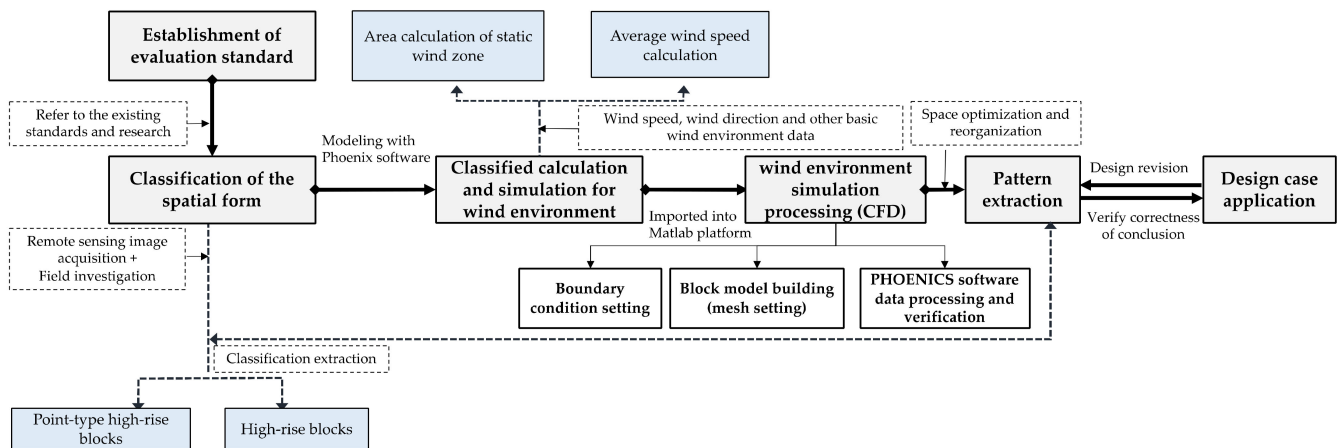


Figure 1. Block diagram of the overall methodology.

2.2.2. Classification of the Spatial Form

The public statistical government document CHANGCHUN STATISTICAL YEARBOOK-2020 shows that HPT and MRT are the main building forms of blocks, accounting for more than 80% of all blocks in the low mountainous areas of Changchun. The main influencing factor for the HPT is the ratio of the street width to the building height, R_{HD} , whereas for the MRT it is the building height [32–34]. Therefore, simulations were conducted for blocks composed of both HPT and MRT, combining the building form with the slope direction and slope intersection of the building to obtain different spatial patterns for simulation and analysis.

2.2.3. Methods of Evaluation and Calculation

(1) Average wind speed and calm wind area ratio

The average wind speed (W_{AS}) and calm wind area ratio (S_{CA}) are important factors affecting the block space wind environment in cold mountainous areas. According to the *Assessment Standard for Green Buildings (GB/T 50378-2019)*, the W_{AS} values of urban residents around the building should not exceed 5 m/s within the human habitat [35–37]. Most cities in China regard 1 m/s as the minimum standard for mitigating the urban heat island effect and the problem of air pollution [38,39]. Creating a comfortable wind environment in block space faces many challenges in low mountainous areas, such as poor human thermal comfort caused by low temperatures in winter and excessive wind speeds [40]. This study combined the upper limits of various standards and norms as an

evaluation basis (Table 1). Second, S_{CA} was used to evaluate the comfortable ratio arc of the block spatial wind environment, calculated according to equation

$$S_{CA} = S_{CC}/S_A \quad (1)$$

Table 1. Relationship between comfort at pedestrian scale and wind speed [41].

Wind Speed (m/s)	Human Feeling
$1 < V < 5$	Comfortable
$5 < V < 10$	Uncomfortable, movement affected
$10 < V < 15$	Very uncomfortable, movement is severely affected
$15 < V < 20$	Cannot stand
$V > 20$	Danger

In this equation, S_{CC} is the area in which the wind speed is within the interval of $1 \text{ m/s} < V_p < 5 \text{ m/s}$, and S_A is the total area of the block.

(2) Mathematical model

In the numerical simulation, air was regarded as an incompressible viscous fluid and the external gas flow was regarded as a steady-state turbulent form. When the air contacted the outer surface of the building a wall-restricted flow was formed; the restricted flow for the wall is expressed using the RNG $k-\epsilon$ Model [42]. As our goal was to apply the results to the block spatial forms for a large scale, the RNG $k-\epsilon$ Model in PHOENICS software was adopted in this study. The standard $k-\epsilon$ model has the advantages of low cost, small numerical fluctuation, and high relative accuracy, and is widely used in the simulation of low-speed turbulence models [42,43]. In the construction of our theoretical model, AutoCAD 2020 and SketchUp 2020 software were used to build the physical model of the urban spatial model and save it as an skp file. The constructed skp model file was imported and parameters such as wind speed, wind direction, and solar radiation were set as shown in Figure 2.

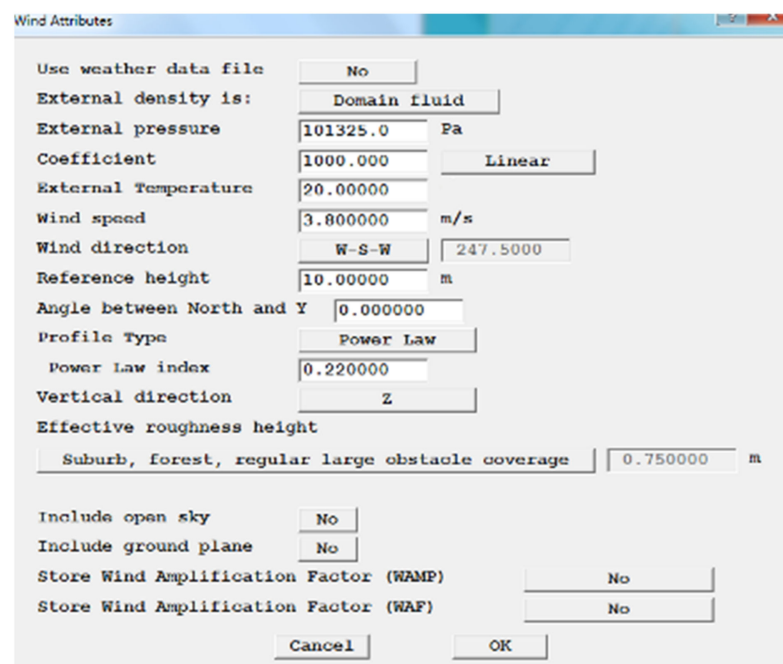


Figure 2. Parameter settings of wind speed and direction.

The boundary conditions should be set according to the actual situation, mainly by including inlet and boundary conditions tailored to accurately represent the elevation dependence of the freestream wind mean velocity and turbulent kinetic energy profiles. Roughness parameters were set to represent the roughness at ground level in the absence of formal representation as block forms, such as for vegetation and objects (Figure 3). In addition, the influencing factors included building height, building density, slope (with the simulation conditions based on an average slope of 5°), slope aspect, and ground roughness. The horizontal wind speed and the calm wind area were the main focus of the investigation.

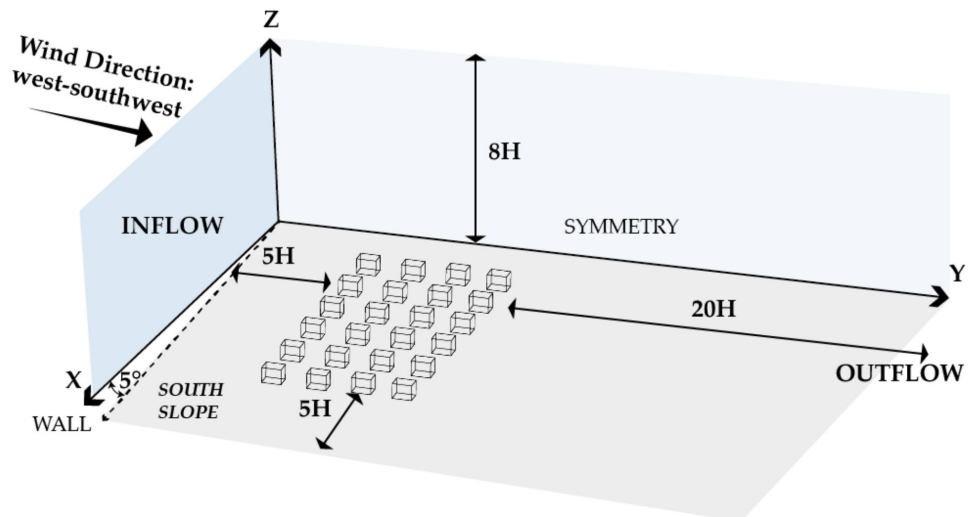


Figure 3. Schematic sketch of the geometry and boundaries used in the simulations (south slope).

To set the inflow boundary conditions, the wind environment of the building group was regarded as an incompressible fluid with different heights of 1.5 m, 10 m, and 20 m. Simultaneously, the roughness of the ground formed a gradient wind. Therefore, the method of exponential relationship analysis and correcting gradient wind was adopted. The equation used in the PHOENICS simulation process is as follows:

$$\frac{U_z}{U_0} = \left(\frac{Z}{Z_0} \right)^\alpha \quad (2)$$

where U_z is the horizontal wind speed at height Z (m/s), U_0 is the wind speed in the horizontal direction of reference height Z_0 (m/s), and α represents Hellman's wind shear component. In keeping with the government standard document Load Code for the Design of Building Structures (GB 50009-2001), the terrain was divided into four categories (Table 2). Changchun belongs to type C, where $\alpha = 0.22$.

Table 2. The α value of different area types.

Classification	Area Type	α Value
A	Coastal areas, islands, lakeshore, or desert areas	0.12
B	Fields, villages or small and medium-sized cities with sparse houses and suburbs of large cities	0.16
C	Urban area with dense buildings	0.22
D	Urban area with extremely dense and high buildings	0.30

(3) Mesh and Boundary condition setting in the simulation

In order to reduce the calculation time and accelerate the convergence speed, the block building model was simplified into a regular cube. According to previous simulation experience, the height of the wind field was set to five times that of the highest building, the length eight times, and the width five times that of the building group.

In addition, the model mesh was set in PHOENICS (see Figure 4). Special attention was paid to achieving near-wall mesh resolution in order to ensure that the first-cell y^+ (the dimensionless length scale) was appropriate at every wall and ground surface. PHOENICS was used to complete the verification process automatically. When the residual value of each variable was less than 10×10^{-5} and tended to be flat with the iterative calculation, the parameters of the model were judged to meet the convergence requirements. After the computer completed the calculation and convergence was proven, the regional wind speed, wind pressure, and other simulation results were exported in the form of 2D images.

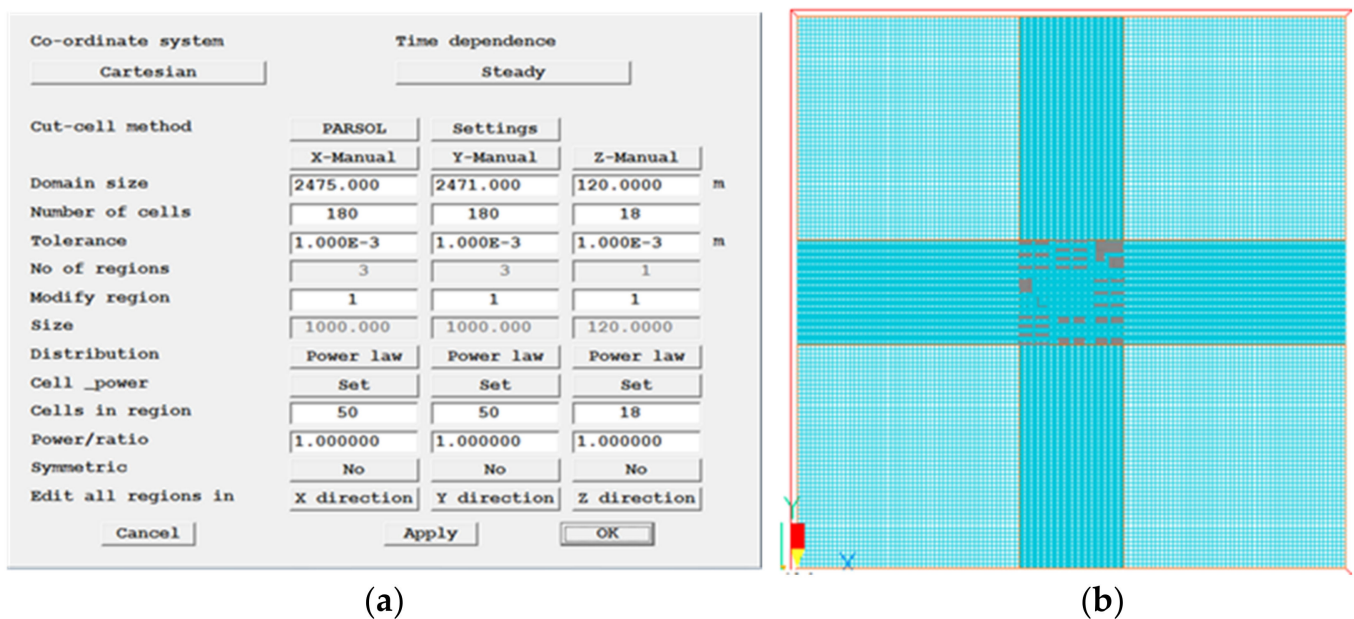


Figure 4. Grid setting: (a) parameter setting of the grid and (b) grid setting layout.

For the outflow boundary condition setting, because the simulation area was smaller than the calculation area of the numerical model in this study the flow restriction on the outlet surface was minimal. Therefore, the outlet boundary condition was set as free outflow. As the top and two sides of the upper surface were far away from the building, the velocity gradient along the tangent direction was set as 0.

Combined with the above mathematical model and condition settings, PHOENICS software was used in this simulation experiment with the following steps. According to the terrain and climate characteristics of the low mountainous area in the cold region of north China, regional factors such as temperature and architectural characteristics were considered when setting influencing factors in order to draw a more rational conclusion with correlation comparisons. The procedure consisted of boundary conditions, experimental validation, and grid-independence analysis.

3. Results and Discussion

3.1. Wind Environment Simulation Results

The building styles and four slope aspects were combined to form different types of spatial patterns. The wind environment simulation was conducted via PHOENICS. Then, the downwind environment of cross-sections with heights of 1.5, 10, and 20 m [44,45] at the pedestrian scale was obtained (see Figure 5, and see Appendix A for detailed results).

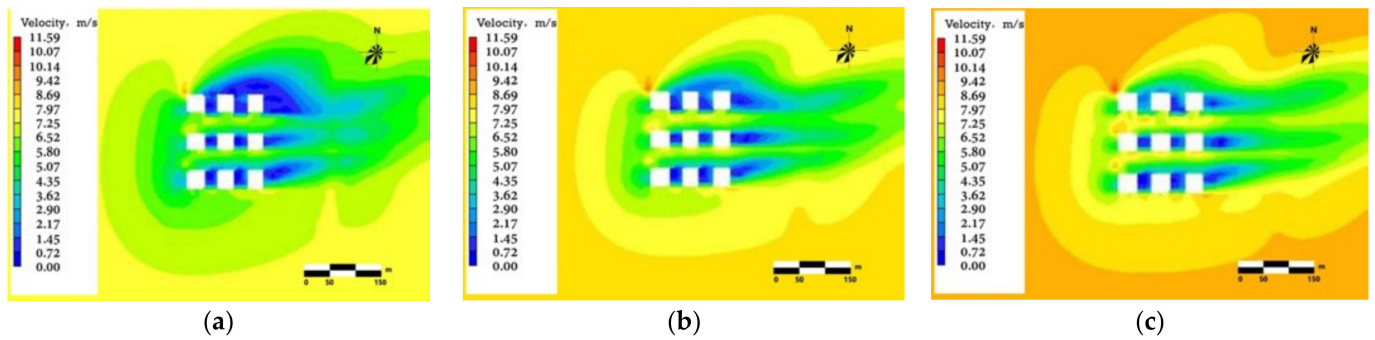


Figure 5. Wind environment simulation at different heights on point-type high-rise buildings (HPT) on the west slope and the street width to building height ratio (1:3): (a) 1.5 m; (b) 10 m; and (c) 20 m.

The simulation results of the wind environment spatial model were compared for different slope aspect conditions in the low mountainous areas of Changchun. The MATLAB platform was used to perform mathematical analysis of the results (Figure 6). The wind environment results of the HPT and MRT were extracted and included the W_{AS} and S_{CA} at heights of 1.5, 10, and 20 m (Tables 3 and 4).

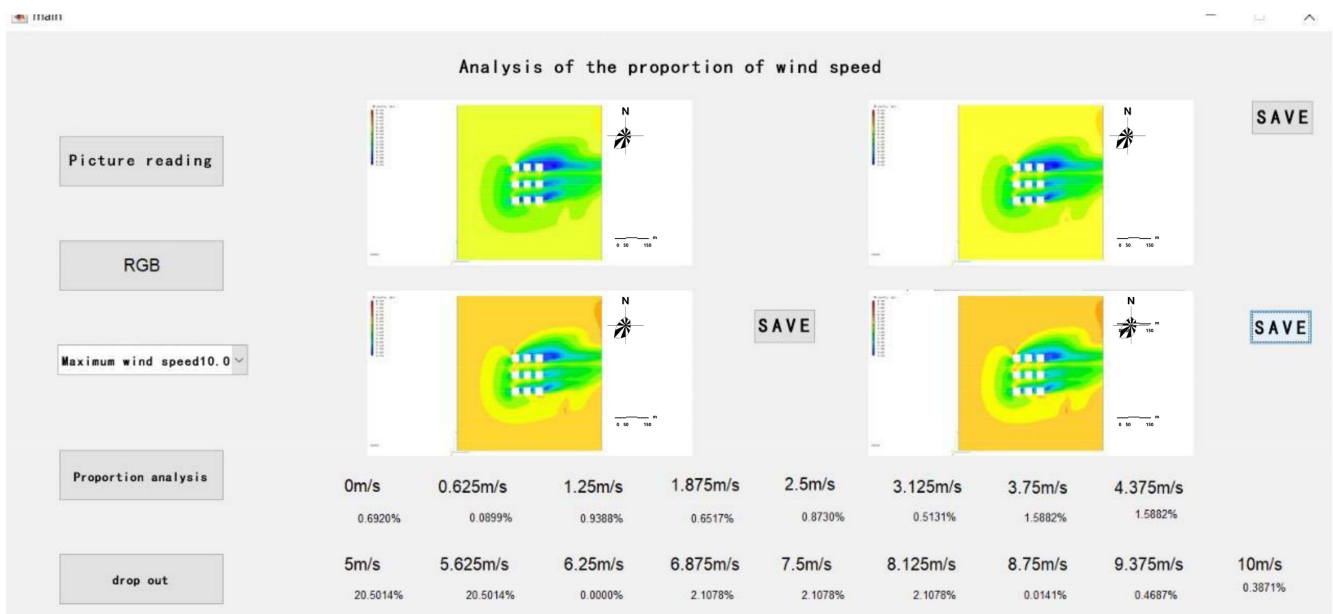


Figure 6. Analysis interface of wind speed ratio based on MATLAB programming.

Table 3. Wind environment simulation results of block composed of point-type high-rise buildings (HPT).

Slope Type	RHD	At a Height of 1.5 m		At a Height of 10 m		At a Height of 20 m	
		W_{AS} (m/s)	S_{CA} %	W_{AS} (m/s)	S_{CA} %	W_{AS} (m/s)	S_{CA} %
Southeast aspect	1:4	2.84	19.6	2.97	18.9	3.46	17.3
	1:3	2.89	20.2	3.12	19.4	3.51	17.8
	1:2	2.94	19.3	3.45	18.7	3.71	16.0
	1:1	3.01	20.4	3.51	19.8	3.80	17.1

Table 3. Cont.

Slope Type	R_{HD}	At a Height of 1.5 m		At a Height of 10 m		At a Height of 20 m	
		W_{AS} (m/s)	S_{CA} %	W_{AS} (m/s)	S_{CA} %	W_{AS} (m/s)	S_{CA} %
South aspect	1:4	2.61	27.3	2.85	24.9	2.91	20.0
	1:3	2.70	27.7	2.87	25.4	2.97	22.5
	1:2	2.74	29.3	2.87	28.9	3.00	23.1
	1:1	3.01	30.4	3.13	29.8	3.22	27.1
Southwest aspect	1:4	2.63	20.3	2.77	19.9	2.86	17.1
	1:3	2.79	23.7	2.92	20.4	3.11	20.0
	1:2	2.84	25.3	2.99	22.9	3.22	21.0
	1:1	3.01	26.4	3.21	25.8	3.30	24.1
West aspect	1:4	2.54	25.3	2.77	23.9	2.96	17.0
	1:3	2.69	27.7	2.72	25.4	3.01	20.0
	1:2	2.84	26.3	2.97	24.9	3.01	22.0
	1:1	2.97	27.4	3.11	24.8	3.20	23.1

Table 4. Wind environment simulation results of block composed of multi-story row-type buildings (MRT).

Slope Type	Building Height (m)	At a Height of 1.5 m		At a Height of 10 m		At a Height of 20 m	
		W_{AS} (m/s)	S_{CA} %	W_{AS} (m/s)	S_{CA} %	W_{AS} (m/s)	S_{CA} %
Southeast aspect	20	2.84	24.3	2.97	23.9	3.06	18.2
	40	2.89	23.7	3.11	22.4	3.19	17.6
	80	2.94	21.3	3.18	20.7	3.24	16.5
South aspect	20	2.54	27.1	2.77	25.9	2.86	23.7
	40	2.59	25.7	2.92	23.4	3.11	22.0
	80	2.54	24.3	2.77	22.9	2.86	20.1
Southwest aspect	20	2.74	25.2	2.87	24.1	2.96	21.0
	40	2.89	22.7	2.92	21.4	3.11	19.7
	80	2.99	20.3	3.17	19.7	3.27	18.0
West aspect	20	2.78	13.3	2.95	11.5	3.04	14.2
	40	2.61	11.5	2.71	10.5	2.95	9.3
	80	2.66	1.4	2.84	1.3	3.01	1.0

3.2. Analysis of Simulation Results

3.2.1. General Relationship between Wind Environment and Block Spatial Form

From the simulation results, with increasing building height the ratio of the horizontal average wind speed to the area of the static wind zone decreased, with the same building form, sloping, and other influencing factors in the low mountainous areas in cold regions; see Figure 7a. Concerning the degree of change, the area ratio of the calm wind area was not completely consistent with the change of the horizontal average wind speed; moreover, the slope aspect affected their relationship. Specifically, the south slope was the least affected and the west slope was the most affected (W_{AS} : south slope > west slope > southwest slope > southeast slope).

With different building heights, the horizontal wind speed of the street space environment changed significantly (see Figure 7b). However, the trend of the change depended on the slope conditions. For example, the horizontal wind speed increased with increasing

building height related to the influence of urban dominant wind direction under the south-east and southwest slope conditions. However, on the west slope, when the building height was less than 40 m the horizontal wind speed decreased with increasing building height. When the building height was more than 40 m, the horizontal wind speed increased with increasing building height. On the south slope, the experimental results were completely different. This reflects the difference between high-rise building blocks and multi-story building blocks.

The experimental results show that there was no direct correlation between S_{CA} and the ratio of the street width to the building height. However, there was a certain relationship between the area ratio of the calm zone and the setting of the building spacing (Figure 7c). Specifically, when the building height ratio was 1:4, the strong wind zone at the pedestrian level occupied a large area, thereby affecting the thermal comfort of residents. Meanwhile, a ratio of 1:2–1:3 both ensured the flow of fresh air to the bottom of the city and reduced the wind speed at the pedestrian height.

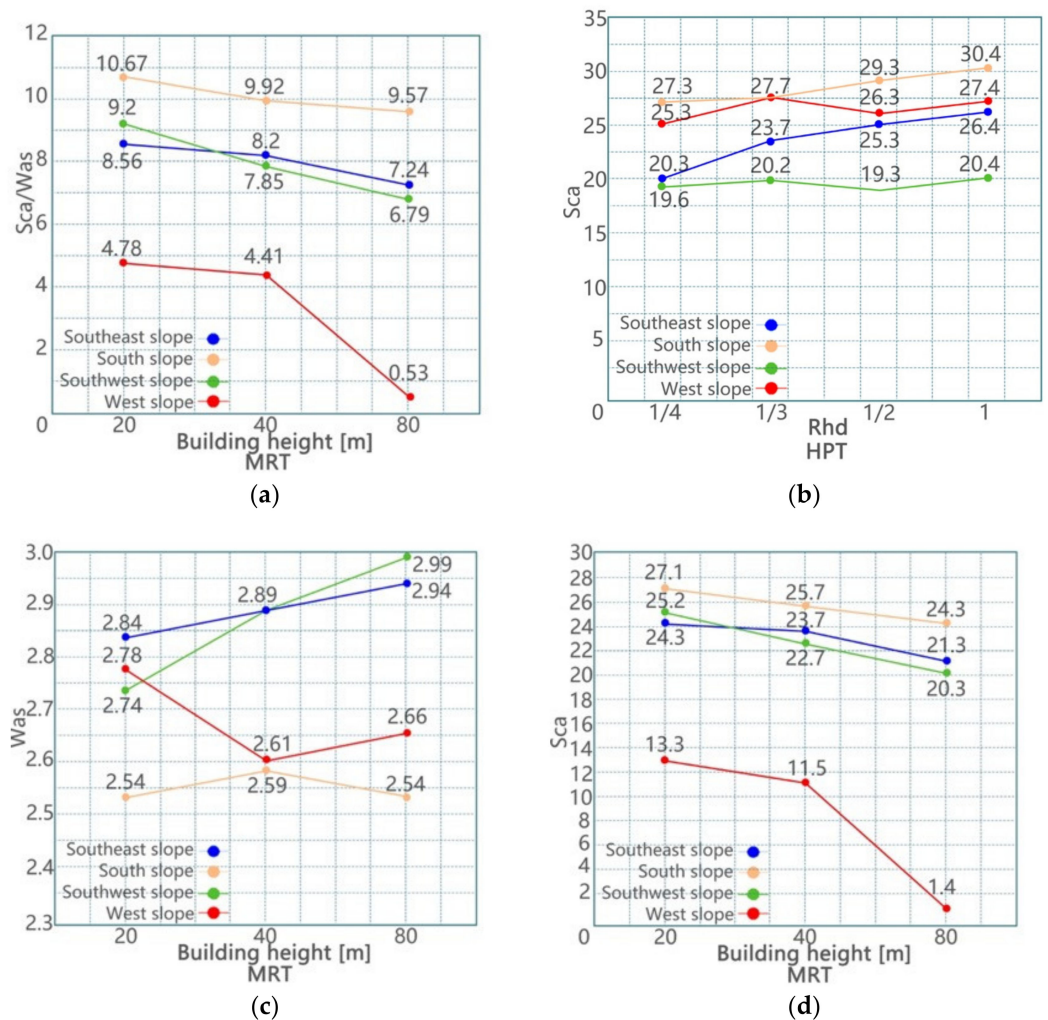


Figure 7. Analysis of simulation results: (a) relationship between building height and S_{CA}/W_{AS} ; (b) relationship between R_{HD} and S_{CA} ; (c) relationship between building height and W_{AS} ; (d) relationship between building height and S_{CA} .

However, for an environment with a certain street width, the ratio of the static wind area in the wind field environment decreased with increasing building height; see Figure 7d. The S_{CA} of the street space on the south slope was the highest, and the comfort of the wind environment was better. The wind environments of the southeast and southwest slopes were similar, with a relatively small difference between them. However, the west slope

conditions affected the area ratio of the calm zone. Especially for high-rise buildings, a greater height resulted in a lower S_{CA} zone at the pedestrian height. Similarly, the area ratio of strong wind areas around the building increased significantly, especially in the corner areas of the building (Figure 7a). This situation seriously affects the thermal comfort of residents.

3.2.2. Optimisation Strategy

(1) Controlling the form of building enclosures

Based on the experimental results, the enclosed form of a street space directly affects its wind environment in cold low mountainous areas. As such, in order to optimise the architectural space form, the enclosure of low-rise buildings can be increased to form a large calm wind area and improve comfort under the climate conditions of cold regions. Specifically, a good ventilation environment in the upper space of the street can be achieved by adopting spatial organisation modes, with the street width and building height in ratios of 1:2 and 1:3. In such a situation, the pedestrian scale wind thermal environment is favourable.

(2) Controlling the building height

When other parameters are constant, a greater the building height, means a smaller ratio of S_{CA} in the wind environment of cold low mountainous areas. Thus, in the block space organisation of cold low mountainous areas, continuous high buildings should be avoided. Moreover, through the simulation analysis of the enclosure forms of different buildings, appropriately improving the enclosure degree of buildings can enhance the area of the calm wind zone. This leads to a more static wind zone appearing, which is useful in urban open space design in cold winter areas.

(3) Controlling the building combination

In designing urban block spaces, the most continuous organisation form of the building group is the main form. In specific areas, such as cold low mountainous areas, the building orientation of the block should be to the southwest. Through this measure the influence of the southwest wind in winter is weakened, ensuring the continuity of the thermal comfort of the block space environment in winter.

3.3. Application of Strategy in Urban Space Planning and Design

The wind environment simulation presented in this study has high practical application value in the urban space design of cold low mountainous areas. The Lianhuashan Ecotourism Resort in Changchun was selected as a case study in this investigation. The resort is located in the low mountainous areas of Changchun and is the future main development area of the city. As the first international ecotourism resort in the city, it has received extensive attention from the government, citizens, and tourists. Therefore, the development and construction of this region are rigorous, especially in the ecological space environment and the comfort of human settlements. The wind environment of the urban space design was simulated based on the master plan, Changchun Lianhuashan Ecotourism Resort (2011–2020).

The elevation data were obtained from field investigations and multispectral unmanned aerial vehicle (Phantom4-RTKCN) measurements. Once the obtained elevation point data were imported into AutoCAD, the elevation point attribute was obtained. Next, the processed elevation data were imported into the SketchUp software to generate the terrain model; see Figure 8a. With the overall project scheme constructed in AutoCAD, SketchUp was used to combine the architectural scheme with the previously built terrain model to form the final experimental model at this stage. The existing scheme model processed by SketchUp for wind environment simulation was imported into PHOENICS in SKP format. MATLAB software was then used to simulate the results. The horizontal average wind speed of the existing scheme was 4.5 m/s, and the area of calm wind accounted for 21.3% of the overall area. According to the combination formed between the four slopes

and the slope directions involved in the previous scheme, the original scheme could be optimised along with the main optimisation areas; see Figure 8b.

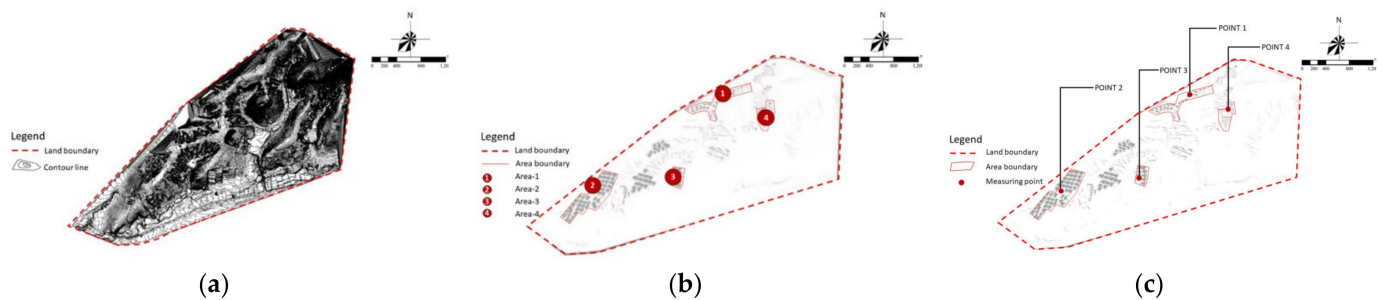


Figure 8. Preparation for simulation: (a) terrain model; (b) main optimisation; (c) validation point.

In order to validate the CFD performance, the wind speed in four areas (points 1–4 in Figure 8c) was measured from 15:30 to 18:30 on 17 February 2022. The test instrument was an anemometer (TESTO 4-10-2). The wind speed at each measuring point was measured for ten groups, each lasting for 10 min. The average wind speed of the groups at each measuring point was obtained according to the average value of 120 data records. Simultaneously, the constructed PHOENICS model was used to simulate the wind speed. The relationship between the measured and simulation results can be seen in Table 5. These findings prove the applicability of the CFD model parameter set in Changchun. First, as the measured data results were affected by the surrounding plants, pedestrians, and even the operators, the software simulation value was generally higher than the measured values, however, it was within the acceptable range. Second, the measured results in the green space (point 4) show that the distribution of high-density plants changed the wind speed significantly.

Table 5. W_{AS} results of physical measurement and simulation results at different points.

POINT	Mode	Physical Measurement (W_{AS})	Simulation Measure (W_{AS})
POINT 1		4.19 m/s	4.21 m/s
POINT 2		3.92 m/s	3.92 m/s
POINT 3		3.61 m/s	3.63 m/s
POINT 4		3.33 m/s	3.38 m/s

Furthermore, with the help of CFD (Figure 9a) it was found that the S_{CA} involved in the plan was less than 20%. Therefore, the wind environment experience of the existing urban space design is relatively poor. Starting from the building enclosure form, height control, and block building organisation, two areas within the plot were selected for the plan revision (Figure 9b). The main correction strategies are as follows.

Area 1 is the southwest slope aspect. The street aspect ratio of the block composed of HPT buildings could be corrected from 1:4 to 1:2. Area 2 is the west slope aspect. The building form is dominated by residential buildings of row-type. Here, 10% of the original high-rise buildings of row-type are reduced to MRT buildings and group houses are set up instead. Using CFD to help simulate the scheme, the average wind speed after revision can be significantly reduced and the area of the calm wind zone significantly increased (see Table 6). Area 3 is a southeast slope aspect, where the original high-rise structure could be reduced to a multi-story building. Area 4 is the south slope aspect, where the original HPT building could see the street width ratio adjusted to 1:2 or 1:3, with which people could experience the best wind environment.

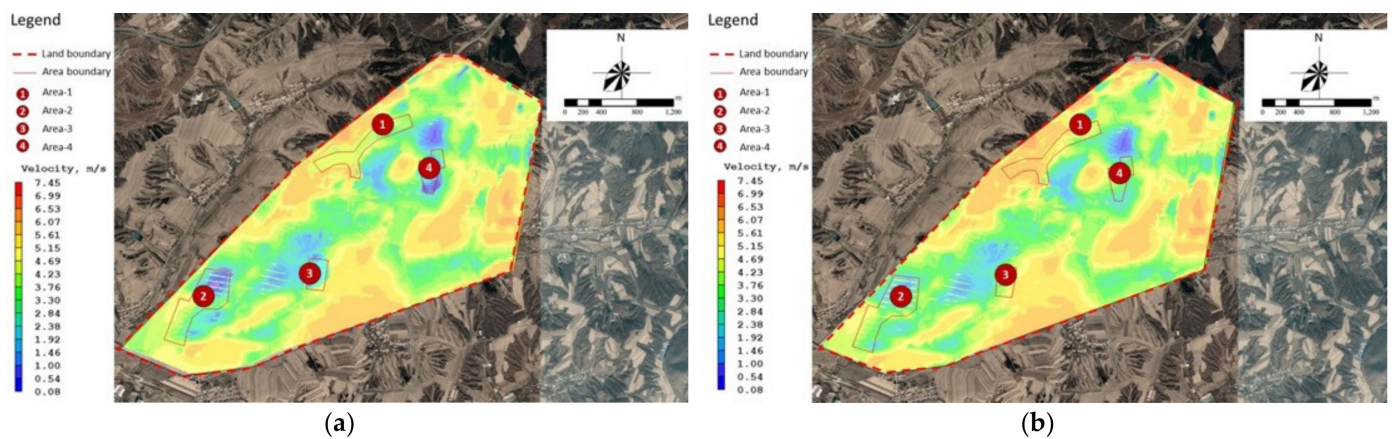


Figure 9. Result of wind environment optimisation: (a) current stage of the plan and (b) after program revision.

Table 6. Comparison results before and after regional wind environment correction.

Area	W _{AS}			S _{CA}		
	Before Correction	After Correction	Decrease	Before Correction	After Correction	Increase
Area 1	4.2 m/s	3.8 m/s	9%	17.1%	21.3%	24%
Area 2	3.9 m/s	3.5 m/s	10%	18.5%	24.1%	30%
Area 3	3.6 m/s	3.3 m/s	8%	19.3%	20.5%	21%
Area 4	3.4 m/s	3.2 m/s	6%	18.2%	22.4%	23%

4. Conclusions

Long winters provide a poor wind environment experience in most cold low mountainous cities. Therefore, the urban block spatial form organisation has a significant impact on the activities, comfort, and spatial experiences of residents. As wind environment research in China is mostly concentrated in South China, research on cold cities, especially those in cold low mountainous areas, has been very limited. Furthermore, research on the combination of wind environment simulation analysis and spatial form construction of cold low mountainous areas is very scarce.

In this study, Changchun, China, which has the key characteristics of a cold city located in low mountainous terrain, was used as an example to solve the important problem of reducing wind speed in winter to improve human comfort. Through a model summary and wind environment simulation analysis of the existing spatial morphology of the low mountainous area in Changchun City and guidance regarding the construction of the spatial morphology of this area, a multi-disciplinary model was developed. First, when the building form, slope direction, and slope were constant, W_{AS} was inversely proportional to S_{CA} , following the order of south slope > west slope > southwest slope > southeast slope. Second, proper selection of 1:2 and 1:3 ratios for HPT buildings can provide good ventilation in the upper layer and the best pedestrian-scale wind environment in cold low mountainous areas. In addition, continuous high-rise buildings should be avoided. The results were integrated into the construction of the spatial morphology of cold low mountainous areas, which were then analysed by controlling the variables. Then, the different slope directions were simulated under the same architectural form.

Combined with CFD simulation analysis, a more accurate relationship between the architecture and space organisation in cold districts was proposed at the pedestrian scale, which can serve as a reference for improving wind environment comfort in space construction in similar areas. Through research on factors such as the street width ratio between buildings, building height, and topographical aspects, the most suitable spatial form for low mountainous areas in cold cities was determined. Moreover, the results of the wind

environment analysis were integrated into the spatial morphology construction of low mountainous areas in Changchun in order to guide this construction.

Due to the similarity of the wind environment characteristics in global cold cities, especially in cold low mountainous areas, the results of this study can be implemented in other areas, and can thus play a guiding role in the construction of spatial forms and the macro-control of cold low mountainous areas.

As the optimisation strategy proposed in this study is based on the wind environment simulation results of typical block types (HPT and MRT) in Changchun, there remain limitations for other block-related strategies. Further research should involve in-depth studies of alternative block types.

Author Contributions: Conceptualisation, H.Z. (Hongyu Zhao) and Y.C.; methodology, Y.C. and X.J.; software, Y.C.; validation, H.Z. (Haina Zhang), S.Z. (Shinan Zhen), R.J. and S.Z. (Shichao Zhang); formal analysis, Y.C.; investigation, Y.C., R.J. and S.Z. (Shichao Zhang); resources, H.Z. (Haina Zhang) and S.Z. (Shinan Zhen); data curation, R.J. and S.Z. (Shichao Zhang); writing—original draft preparation, Y.C. and X.J.; writing—review and editing, X.J.; visualisation, H.Z. (Haina Zhang), S.Z. (Shinan Zhen), R.J. and S.Z. (Shichao Zhang); supervision, H.Z. (Hongyu Zhao); project administration, H.Z. (Hongyu Zhao) and X.J.; funding acquisition, H.Z. (Hongyu Zhao) and X.J. All authors have read and agreed to the published version of the manuscript.

Funding: This research was funded by the National Natural Science Foundation of China (grant number 52178042), the Technology Research Project of Jilin Provincial Department of Education in China (grant number JJKH20220299KJ), and Key projects of Jilin Provincial Department of Science and Technology (grant number 20210203213SF).

Institutional Review Board Statement: Not applicable.

Informed Consent Statement: Not applicable.

Data Availability Statement: Not applicable.

Conflicts of Interest: The authors declare no conflict of interest.

Appendix A

Table A1. Wind simulation results for HPT at different R_{HD} and heights (southeast slope aspect).

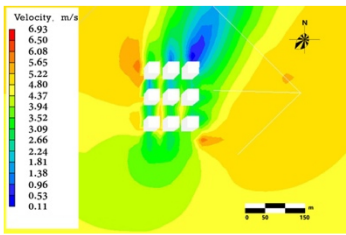
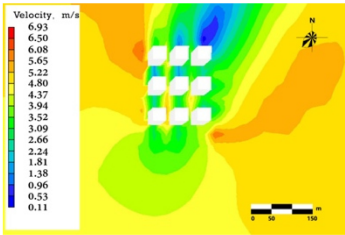
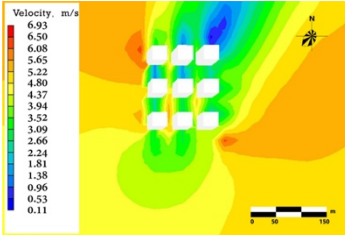
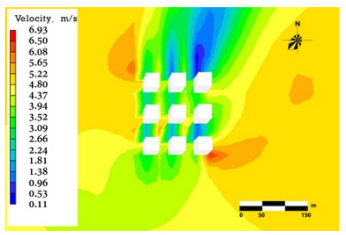
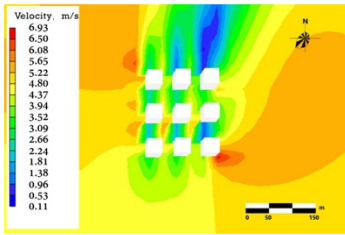
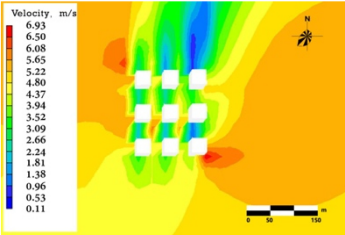
R_{HD}	1.5 m	10 m	20 m
1:4	 <p>W_{AS}: 2.84 m/s S_{CA}: 19.6%</p>	 <p>W_{AS}: 2.97 m/s S_{CA}: 18.9%</p>	 <p>W_{AS}: 3.46 m/s S_{CA}: 17.3%</p>
1:3	 <p>W_{AS}: 2.89 m/s S_{CA}: 20.2%</p>	 <p>W_{AS}: 3.12 m/s S_{CA}: 19.4%</p>	 <p>W_{AS}: 3.51 m/s S_{CA}: 17.8%</p>

Table A1. Cont.

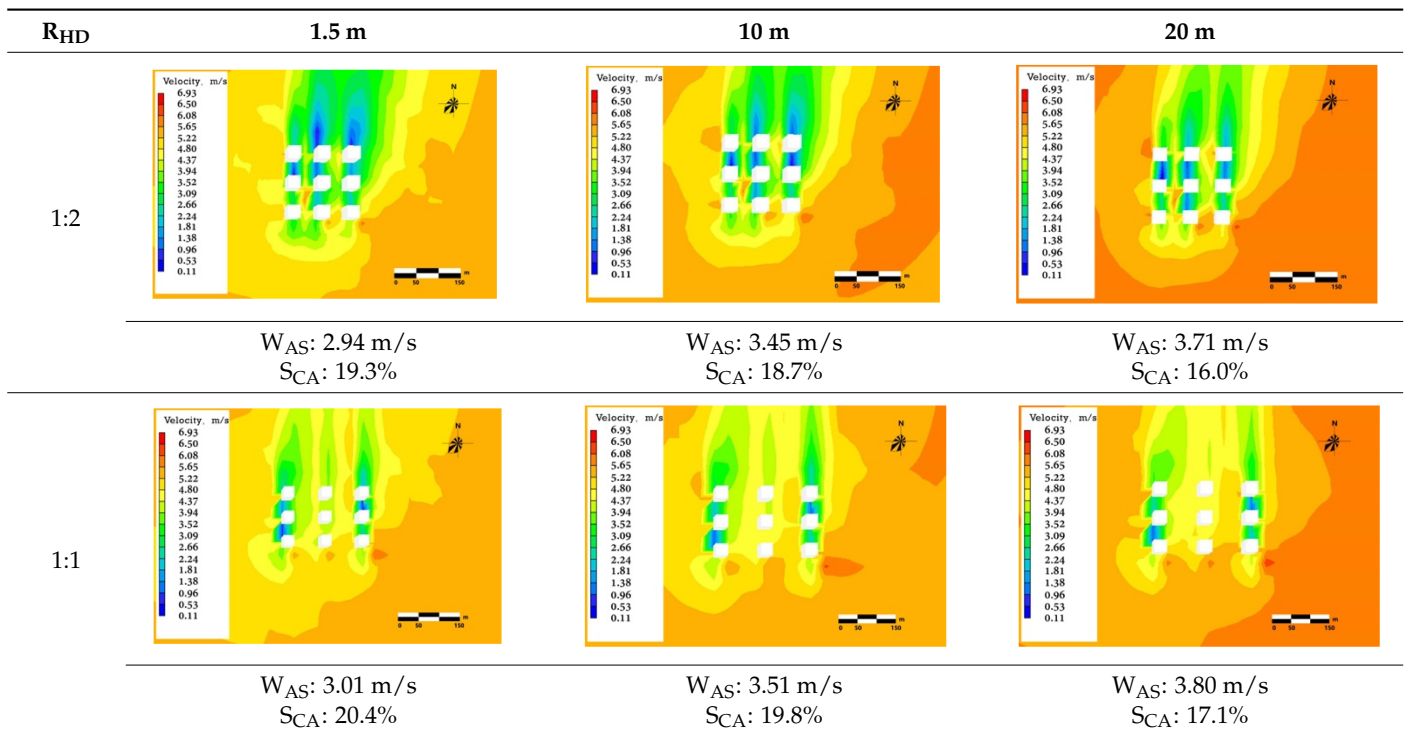


Table A2. Wind simulation results for HPT at different R_{HD} and heights (south slope aspect).

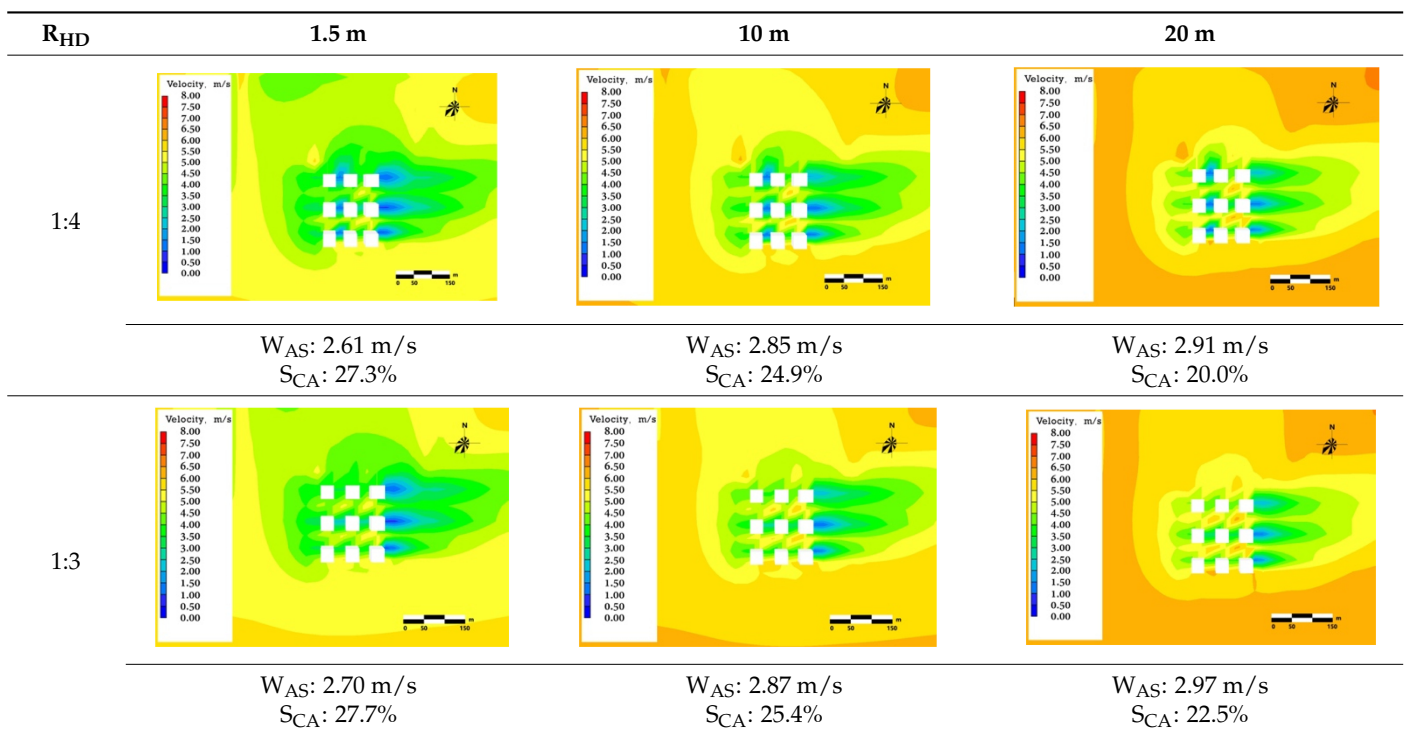


Table A2. Cont.

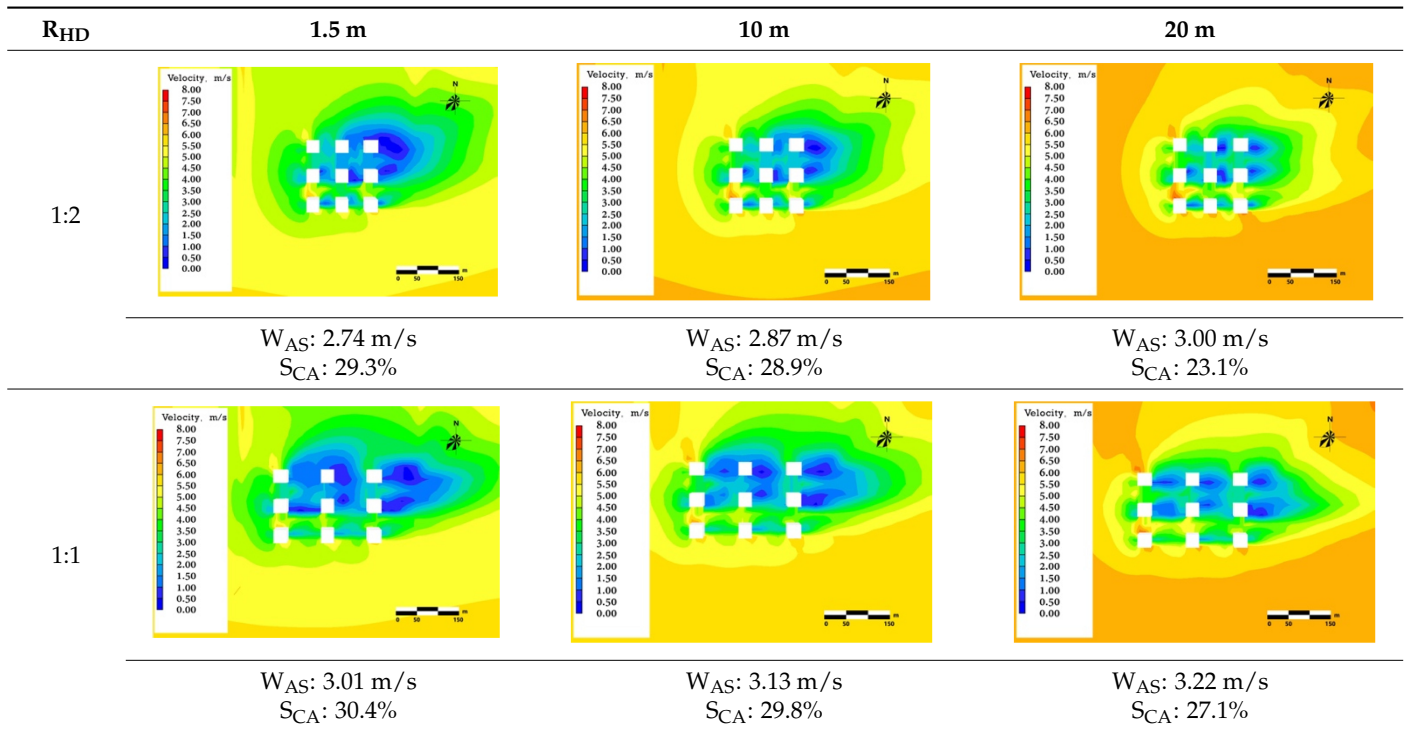


Table A3. Wind simulation results for HPT at R_{HD} and heights (southwest slope aspect).

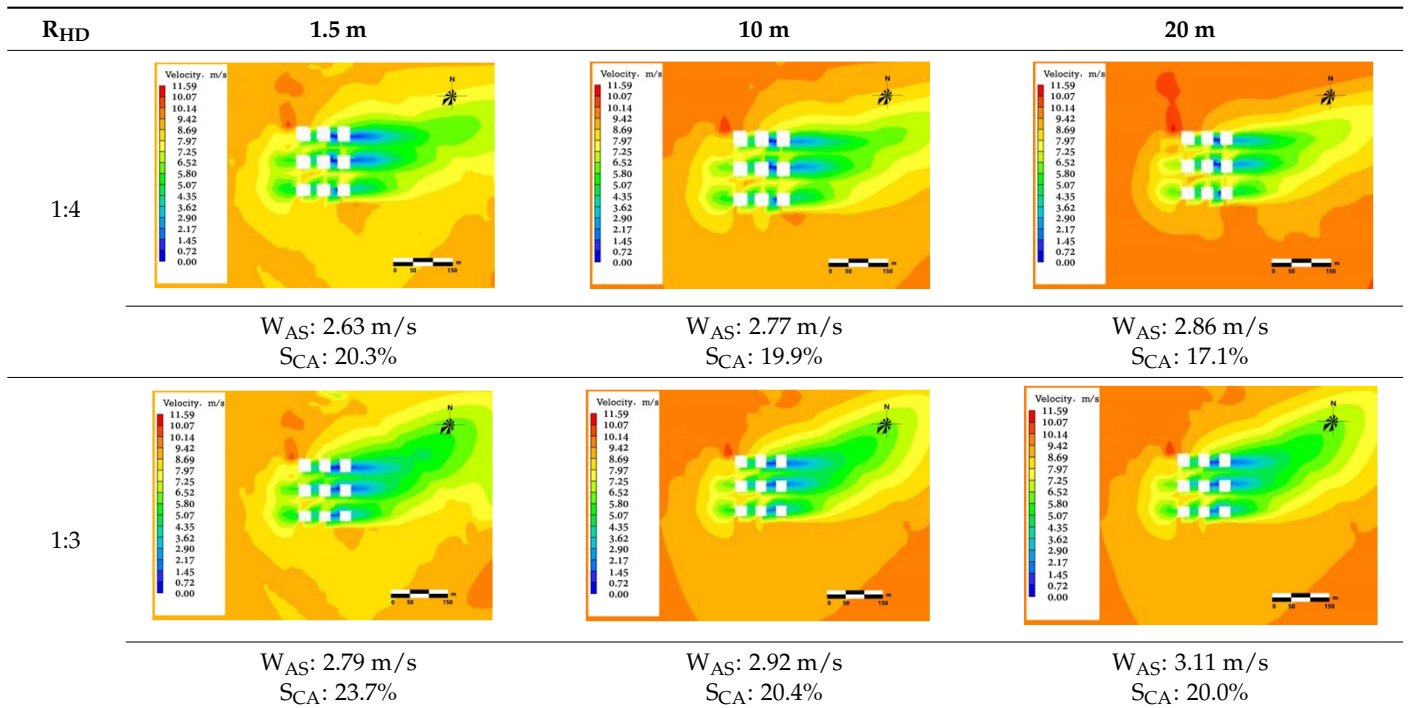


Table A3. Cont.

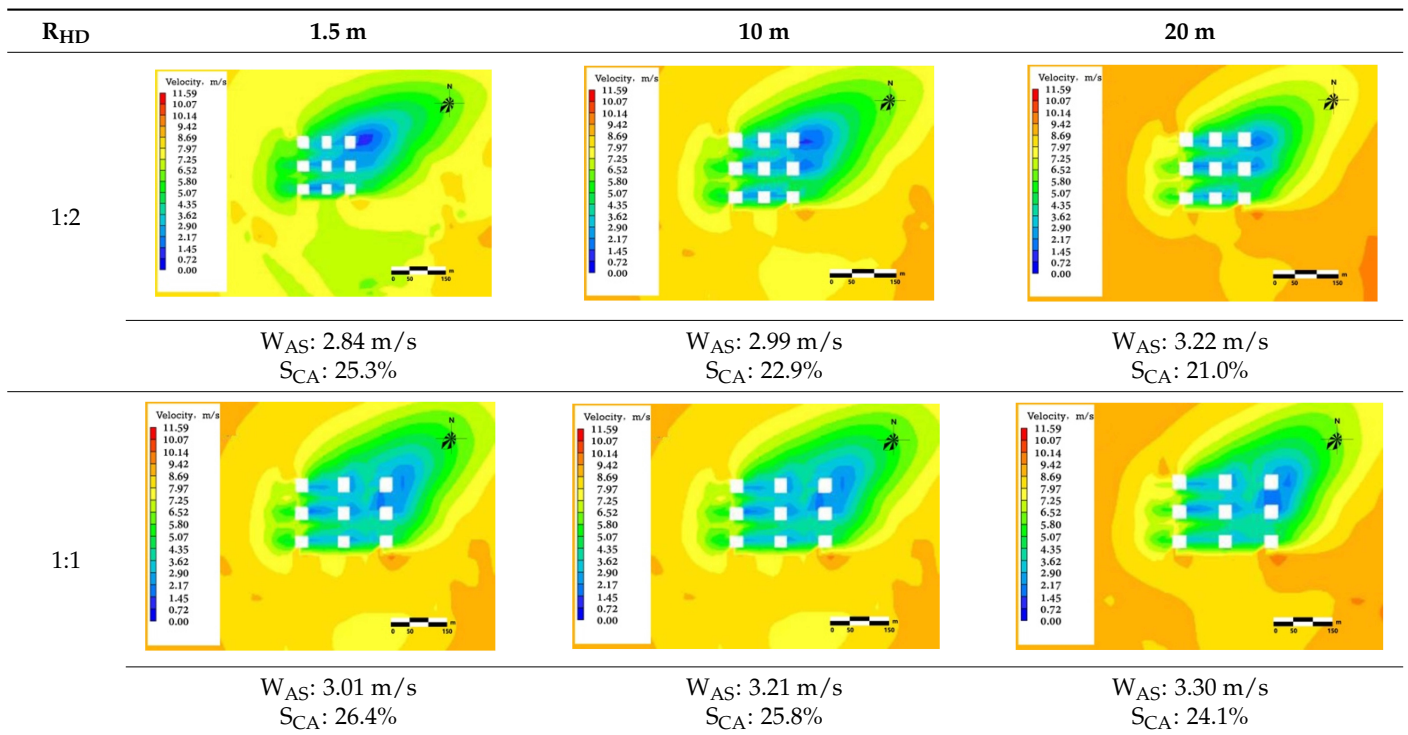


Table A4. Wind simulation results for HPT at different R_{HD} and heights (west slope aspect).

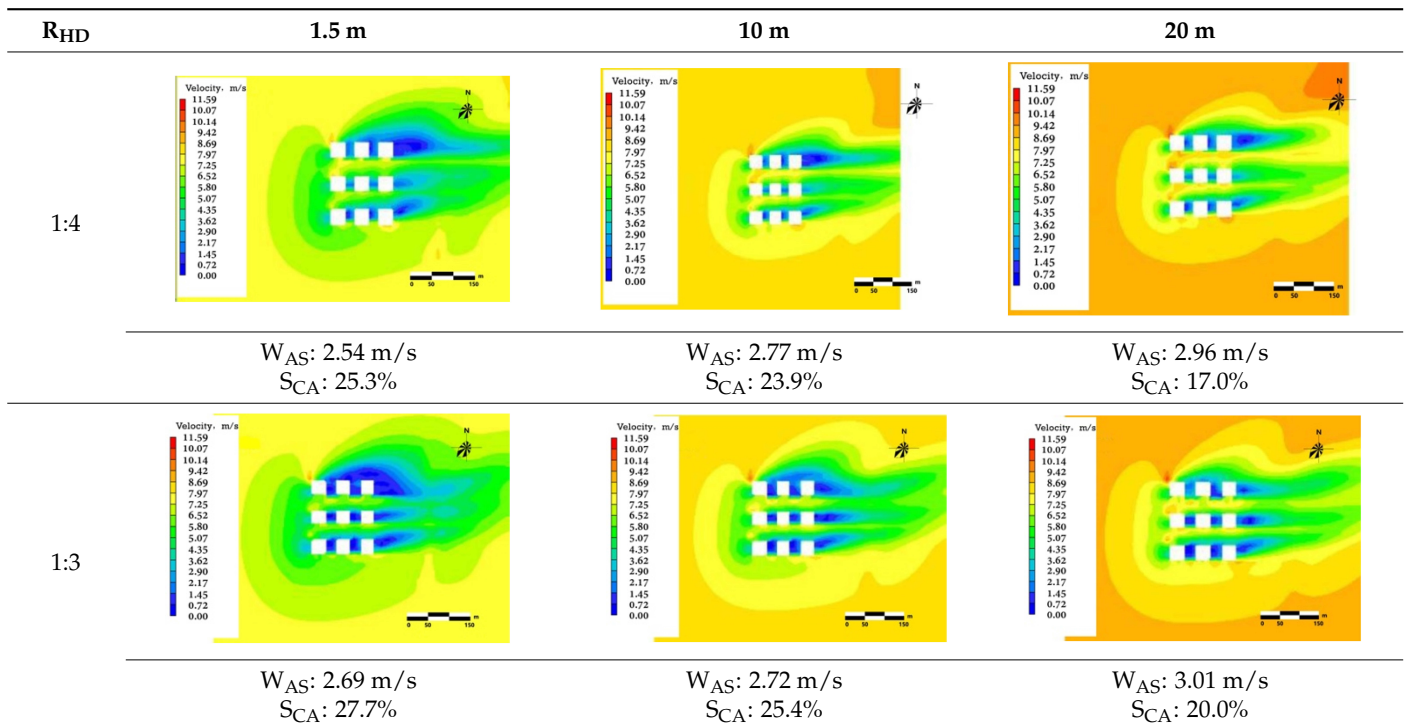


Table A4. Cont.

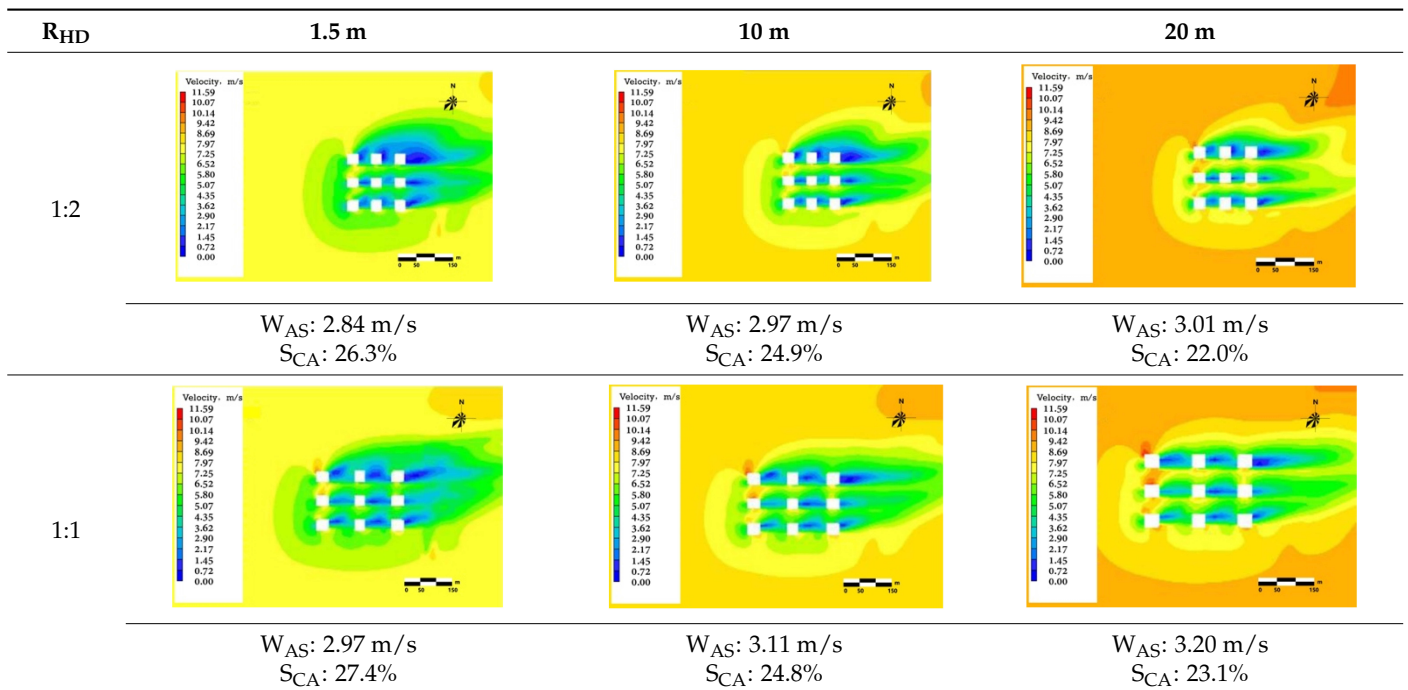


Table A5. Wind simulation results for MRT at different heights (southeast slope aspect).

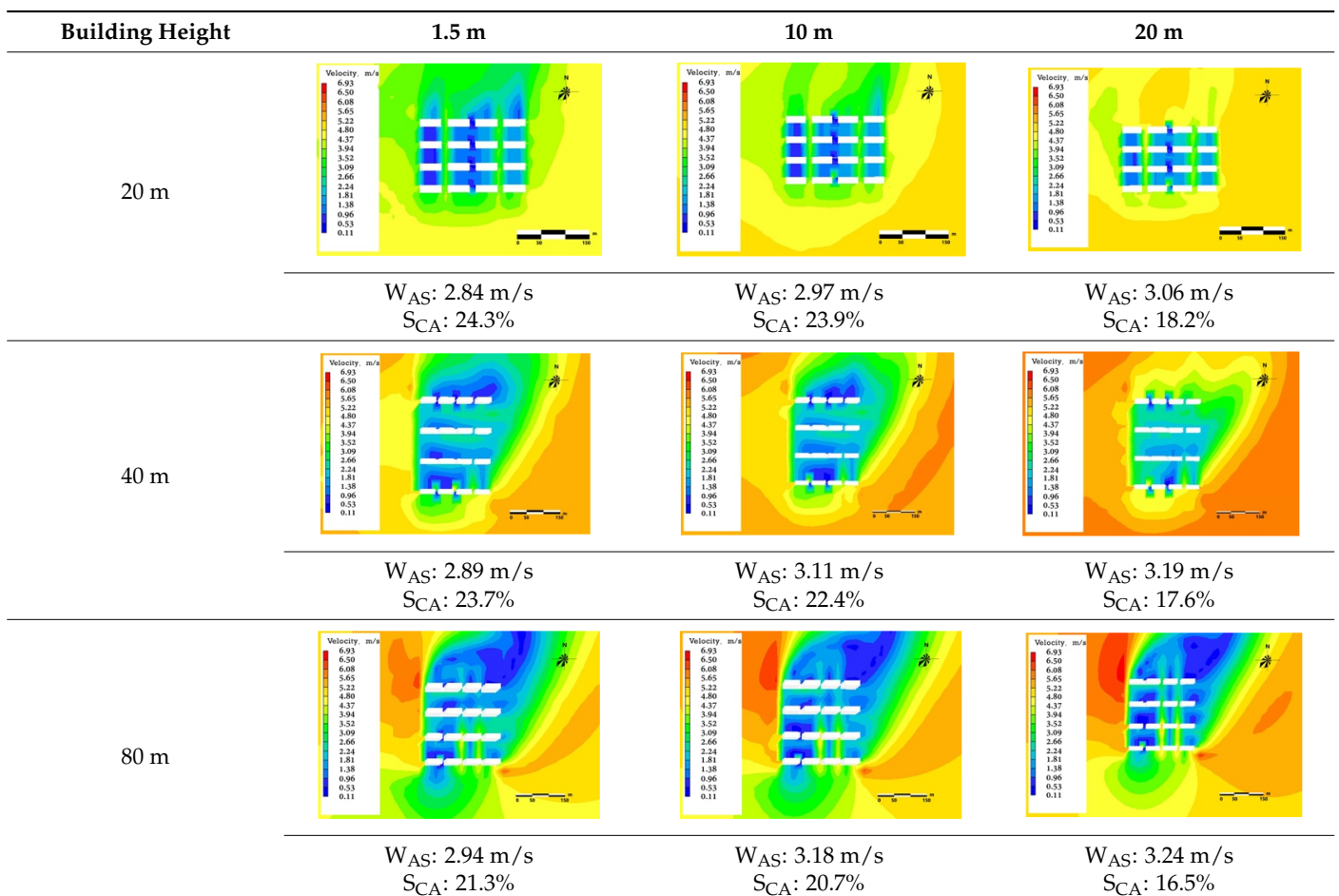


Table A6. Wind simulation results of MRT at different heights (south slope aspect).

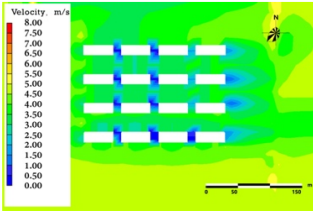
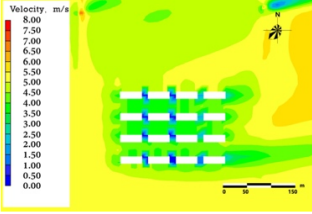
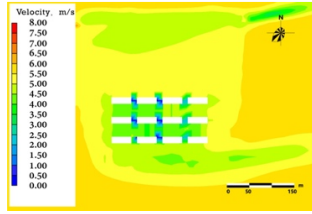
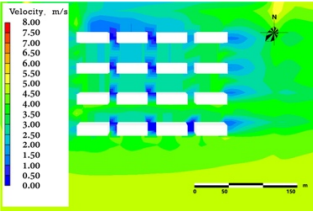
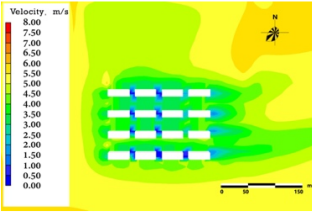
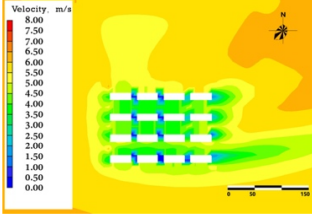
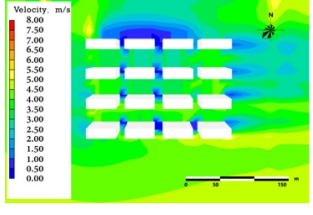
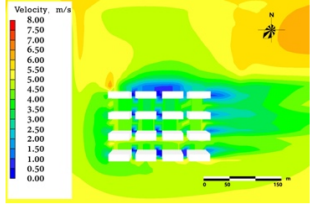
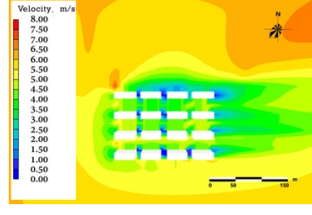
Building Height	1.5 m	10 m	20 m
20 m			
	$W_{AS}: 2.54 \text{ m/s}$ $SCA: 27.1\%$	$W_{AS}: 2.77 \text{ m/s}$ $SCA: 25.9\%$	$W_{AS}: 2.86 \text{ m/s}$ $SCA: 23.7\%$
40 m			
	$W_{AS}: 2.59 \text{ m/s}$ $SCA: 25.7\%$	$W_{AS}: 2.92 \text{ m/s}$ $SCA: 23.4\%$	$W_{AS}: 3.11 \text{ m/s}$ $SCA: 22.0\%$
80 m			
	$W_{AS}: 2.54 \text{ m/s}$ $SCA: 24.3\%$	$W_{AS}: 2.77 \text{ m/s}$ $SCA: 22.9\%$	$W_{AS}: 2.86 \text{ m/s}$ $SCA: 20.1\%$

Table A7. Wind simulation results for MRT at different heights (southwest slope aspect).

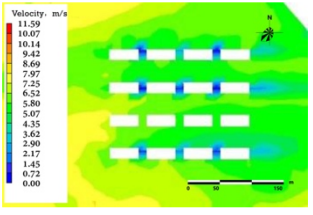
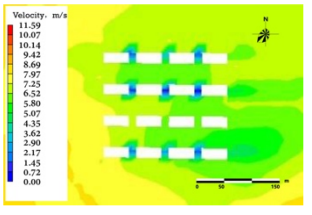
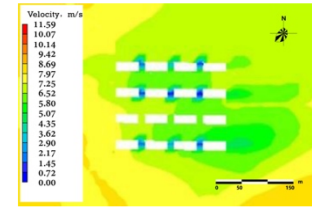
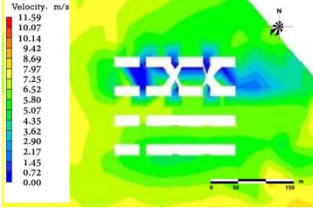
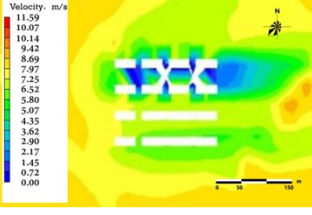
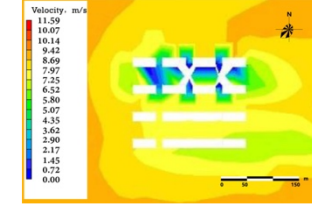
Building Height	1.5 m	10 m	20 m
20 m			
	$W_{AS}: 2.74 \text{ m/s}$ $SCA: 25.2\%$	$W_{AS}: 2.87 \text{ m/s}$ $SCA: 24.1\%$	$W_{AS}: 2.96 \text{ m/s}$ $SCA: 21.0\%$
40 m			
	$W_{AS}: 2.89 \text{ m/s}$ $SCA: 22.7\%$	$W_{AS}: 2.92 \text{ m/s}$ $SCA: 21.4\%$	$W_{AS}: 3.11 \text{ m/s}$ $SCA: 19.7\%$

Table A7. Cont.

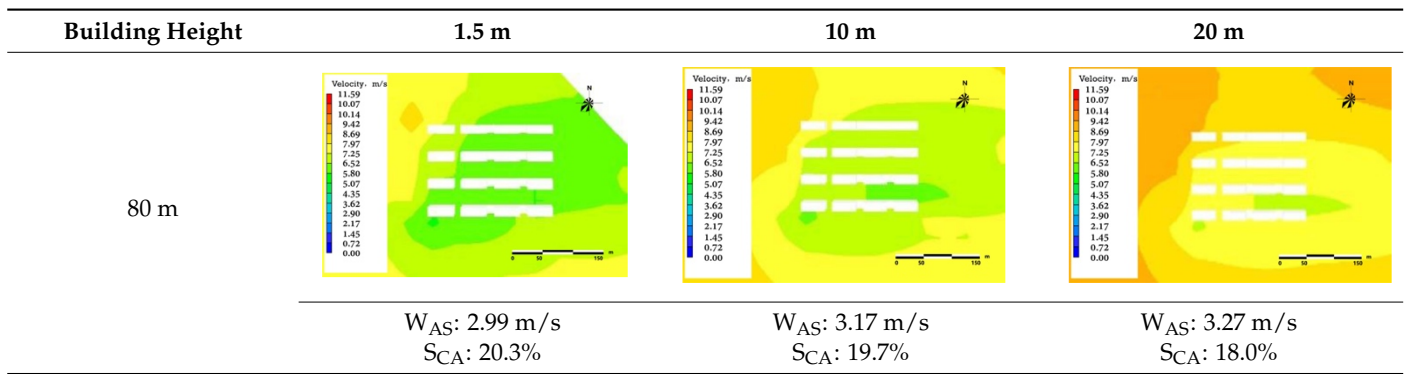
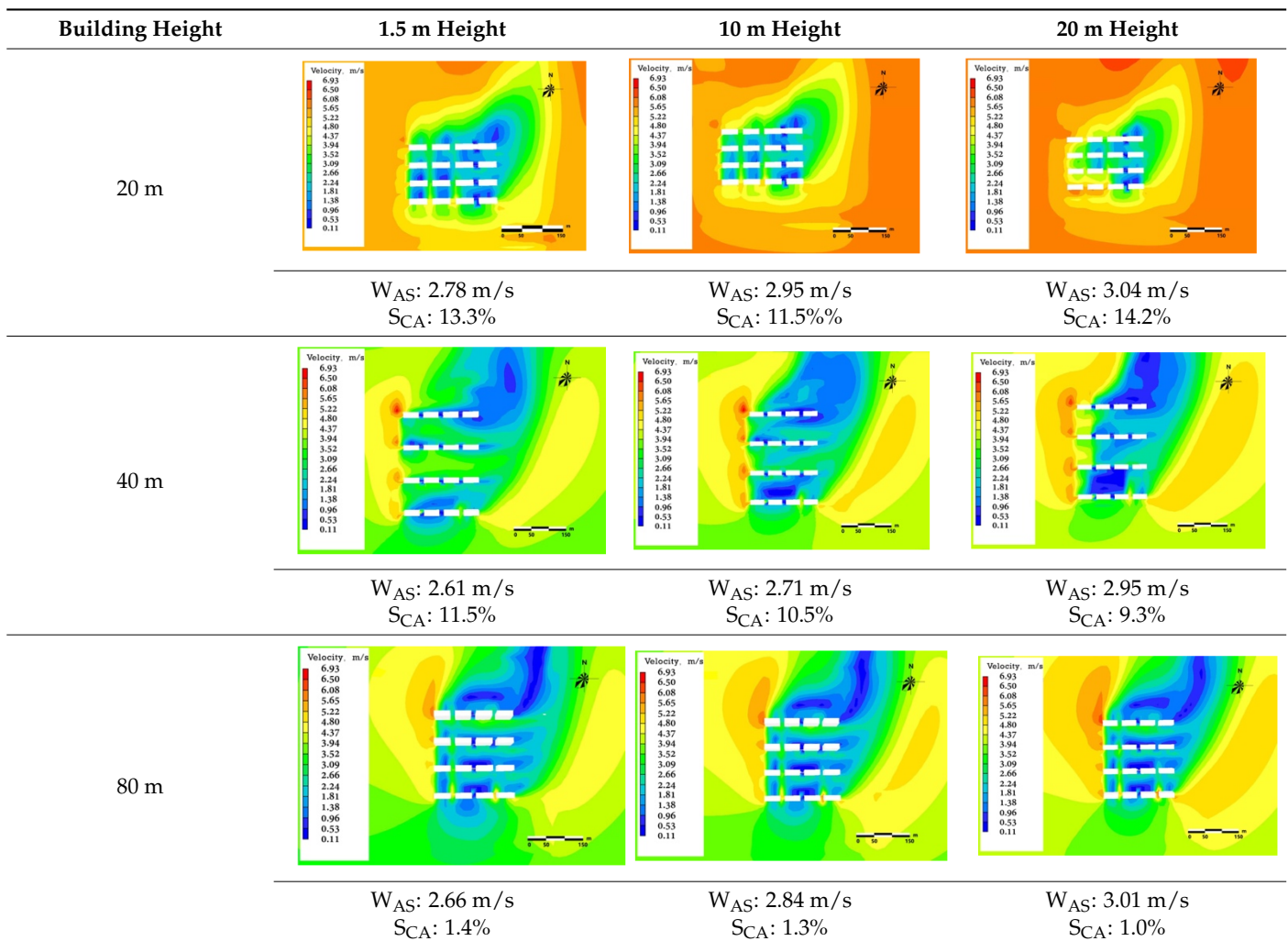


Table A8. Wind simulation results for MRT at different heights (west slope aspect).



References

1. Yu, K.; Yuan, H.; Li, D.; Wang, S.; Qiao, Q. Difficulties and solutions of sustainable land use in shallow hilly area of Beijing. *China Land Sci.* **2009**, *23*, 3–8, 20.
2. Bai, L.; Xiu, C.; Feng, X.; Liu, D. Influence of urbanization on regional habitat quality: A case study of Changchun City. *Habitat Int.* **2019**, *93*, 102042. [[CrossRef](#)]
3. Li, G.; Jiang, C.; Du, J.; Jia, Y.; Bai, J. Spatial differentiation characteristics of internal ecological land structure in rural settlements and its response to natural and socio-economic conditions in the Central Plains, China. *Sci. Total Environ.* **2020**, *709*, 135932. [[CrossRef](#)]
4. Kaur, H.; Garg, P. City profile: New Tehri. *Cities* **2020**, *102*, 102718. [[CrossRef](#)]
5. Wang, F.; Wang, Y. Potential role of local contributions to record-breaking high-temperature event in Xiamen, China. *Weather Clim. Extrem.* **2021**, *33*, 100338. [[CrossRef](#)]
6. Chen, Z.; Liu, Y.; Feng, W.; Li, Y.; Li, L. Study on spatial tropism distribution of rural settlements in the Loess Hilly and Gully Region based on natural factors and traffic accessibility. *J. Rural Stud.* **2019**, *2*, 14. [[CrossRef](#)]
7. Liu, J.; Niu, J. CFD simulation of the wind environment around an isolated high-rise building: An evaluation of SRANS, LES and DES models. *Build. Environ.* **2016**, *96*, 91–106. [[CrossRef](#)]
8. Kikumoto, H.; Choi, W.; Ooka, R. Development of probabilistic assessment framework for pedestrian wind environment using Bayesian technique. *Build. Environ.* **2021**, *187*, 107419. [[CrossRef](#)]
9. Weerasuriya, A.U.; Hu, Z.Z.; Zhang, X.L.; Tse, K.T.; Li, S.; Chan, P.W. New inflow boundary conditions for modeling twisted wind profiles in CFD simulation for evaluating the pedestrian-level wind field near an isolated building. *Build. Environ.* **2018**, *132*, 303–318. [[CrossRef](#)]
10. Zhang, S.; Kwok, K.C.S.; Liu, H.; Jiang, Y.; Dong, K.; Wang, B. A CFD study of wind assessment in urban topology with complex wind flow. *Sustain. Cities Soc.* **2021**, *71*, 103006. [[CrossRef](#)]
11. Buccolieri, R.; Sandberg, M.; Di Sabatino, S. City breathability and its link to pollutant concentration distribution within urban-like geometries. *Atmos. Environ.* **2010**, *44*, 1894–1903. [[CrossRef](#)]
12. Hang, J.; Wang, Q.; Chen, X.; Sandberg, M.; Zhu, W.; Buccolieri, R.; Di Sabatino, S. City breathability in medium density urban-like geometries evaluated through the pollutant transport rate and the net escape velocity. *Build. Environ.* **2015**, *94*, 166–182. [[CrossRef](#)]
13. Hågbo, T.; Giljarhus, K.E.T.; Hjertager, B.H. Influence of geometry acquisition method on pedestrian wind simulations. *J. Wind Eng. Ind. Aerodyn.* **2021**, *215*, 104665. [[CrossRef](#)]
14. Du, Y.; Mak, C.M.; Kwok, K.; Tse, K.T.; Lee, T.; Ai, Z.; Liu, J.; Niu, J. New criteria for assessing low wind environment at pedestrian level in Hong Kong. *Build. Environ.* **2017**, *123*, 23–36. [[CrossRef](#)]
15. Acero, J.A.; Arrizabalaga, J.; Kupski, S.; Katzschner, L. Deriving an Urban Climate Map in Coastal Areas with Complex Terrain in the Basque Country (Spain). *Urban Clim.* **2013**, *4*, 35–60. [[CrossRef](#)]
16. Hassan, A.M.; Megahed, N.A. COVID-19 and urban spaces: A new integrated CFD approach for public health opportunities. *Build. Environ.* **2021**, *204*, 108131. [[CrossRef](#)]
17. Jing, Y.; Zhong, H.; Wang, W.; He, Y.; Zhao, F.; Li, Y. Quantitative city ventilation evaluation for urban canopy under heat island circulation without geostrophic winds: Multi-scale CFD model and parametric investigations. *Build. Environ.* **2021**, *196*, 107793. [[CrossRef](#)]
18. Yuan, C.; Adelia, A.S.; Mei, S.; He, W.; Li, X.; Norford, L. Mitigating intensity of urban heat island by better understanding on urban morphology and anthropogenic heat dispersion. *Build. Environ.* **2020**, *176*, 106876. [[CrossRef](#)]
19. Kubota, T.; Miura, M.; Tominaga, Y.; Mochida, A. Wind tunnel tests on the relationship between building density and pedestrian-level wind velocity: Development of guidelines for realizing acceptable wind environment in residential neighborhoods. *Build. Environ.* **2008**, *43*, 1699–1708. [[CrossRef](#)]
20. Li, Z.; Luo, D.; Shi, W.; Li, Z.; Liang, X. Field measurement of wind-induced stress on glass facade of a coastal high-rise building. *Sci. China Technol.* **2011**, *54*, 2587. [[CrossRef](#)]
21. Jia, S.; Wang, Y. Effect of heat mitigation strategies on thermal environment, thermal comfort, and walkability: A case study in Hong Kong. *Build. Environ.* **2021**, *201*, 107988. [[CrossRef](#)]
22. Aflaki, A.; Mirnezhad, M.; Ghaffarianhoseini, A.; Ghaffarianhoseini, A.; Omrany, H.; Wang, Z.; Akbari, H. Urban heat island mitigation strategies: A state-of-the-art review on Kuala Lumpur, Singapore and Hong Kong. *Cities* **2017**, *62*, 131–145. [[CrossRef](#)]
23. Yoshie, R.; Mochida, A.; Tominaga, Y.; Kataoka, H.; Harimoto, K.; Nozu, T.; Shirasawa, T. Cooperative project for CFD prediction of pedestrian wind environment in the Architectural Institute of Japan. *J. Wind Eng. Ind. Aerodyn.* **2007**, *95*, 1551–1578. [[CrossRef](#)]
24. Huang, S.; Li, Q.S.; Xu, S. Numerical evaluation of wind effects on a tall steel building by CFD. *J. Constr. Steel Res.* **2007**, *63*, 612–627. [[CrossRef](#)]
25. Krastev, V.; Silvestri, L.; Bella, G. Effects of Turbulence Modeling and Grid Quality on the Zonal URANS/LES Simulation of Static and Reciprocating Engine-Like Geometries. *SAE Int. J. Engines* **2018**, *11*, 669–686. [[CrossRef](#)]
26. Stefan, H. A review of hybrid RANS-LES methods for turbulent flows: Concepts and applications. *Prog. Aerosp. Sci.* **2020**, *114*, 100697.
27. Mei, S.; Luo, Z.; Zhao, F.; Wang, H. Street canyon ventilation and airborne pollutant dispersion: 2-D versus 3-D CFD simulations. *Sustain. Cities Soc.* **2019**, *50*, 101700. [[CrossRef](#)]

28. Peng, Y.; Gao, Z.; Buccolieri, R.; Shen, J.; Ding, W. Urban ventilation of typical residential streets and impact of building form variation. *Sustain. Cities Soc.* **2021**, *67*, 102735. [[CrossRef](#)]
29. Hadavi, M.; Pasharshahri, H. Quantifying impacts of wind speed and urban neighborhood layout on the infiltration rate of residential buildings. *Sustain. Cities Soc.* **2020**, *53*, 101887. [[CrossRef](#)]
30. Ramponi, R.; Blocken, B.; De Coo, L.B.; Janssen, W.D. CFD simulation of outdoor ventilation of generic urban configurations with different urban densities and equal and unequal street widths. *Build. Environ.* **2015**, *92*, 152–166. [[CrossRef](#)]
31. Ma, T.; Chen, T. Classification and pedestrian-level wind environment assessment among Tianjin’s residential area based on numerical simulation. *Urban. Clim.* **2020**, *34*, 100702. [[CrossRef](#)]
32. Johansson, E.; Emmanuel, R. The influence of urban design on outdoor thermal comfort in the hot, humid city of Colombo, Sri Lanka. *Int. J. Biometeorol.* **2006**, *51*, 119–133. [[CrossRef](#)]
33. Xu, M.; Hong, B.; Mi, J.; Yan, S. Outdoor thermal comfort in an urban park during winter in cold regions of China. *Sustain. Cities Soc.* **2018**, *43*, 208–220. [[CrossRef](#)]
34. Guo, F.; Zhu, P.; Wang, S.; Duan, D.; Jin, Y. Improving Natural Ventilation Performance in a High-Density Urban District: A Building Morphology Method. *Procedia Eng.* **2017**, *205*, 952–958. [[CrossRef](#)]
35. Gamero-Salinas, J.; Kishnani, N.; Monge-Barrio, A.; López-Fidalgo, J.; Sánchez-Ostiz, A. The influence of building form variables on the environmental performance of semi-outdoor spaces. A study in mid-rise and high-rise buildings of Singapore. *Energy Build.* **2021**, *230*, 110544. [[CrossRef](#)]
36. Liu, J.; Niu, J.; Du, Y.; Mak, C.; Zhang, Y. LES for pedestrian level wind around an idealized building array—Assessment of sensitivity to influencing parameters. *Sustain. Cities Soc.* **2019**, *44*, 406–415. [[CrossRef](#)]
37. Cao, Q.; Luan, Q.; Liu, Y.; Wang, R. The effects of 2D and 3D building morphology on urban environments: A multi-scale analysis in the Beijing metropolitan region. *Build. Environ.* **2021**, *192*, 107635. [[CrossRef](#)]
38. Ping, Z.S. *Optimization and CFD Analysis of Urban Wind Environment Based on “Source Flow Sink” Theory*; Tianjin University: Tianjin, China, 2016.
39. Yangyang, Q. *Numerical Simulation of the Influence of Underlying Surface Obstacles on Observation Environment*; Nanjing University of Information Engineering: Nanjing, China, 2013.
40. Yuhang, D. *Research on Wind Environment of Courtyards with Different Enclosure*; Guangzhou University: Guangzhou, China, 2019.
41. Liu, Q.; Liu, B.; Wang, X.; Wang, F.; Wang, C.; Bureau, C. Application of WRF-ARW model in simulation of urban heat island in Beijing. *Sci. Technol. Eng.* **2014**, *14*, 146–151, 164.
42. Richards, P.J.; Hoxey, R.P. Appropriate boundary conditions for computational wind engineering models using the k- ϵ turbulence model. *J. Wind. Eng. Ind. Aerodyn.* **1993**, *46*, 145–153. [[CrossRef](#)]
43. Michael, D.G.; Everett, J.; John, D.A. A computational fluid dynamic technique valid at the centerline for non-axisymmetric problems in cylindrical coordinates. *J. Comput. Phys.* **1979**, *30*, 352–360.
44. Yaxin, W.; Jing, Z. *Discussion on the Demonstration Method of Height Adjustment Based on Wind Environment Optimization-Taking the Demonstration of Height Adjustment of Fudi Yuxiang Mountainous in Tianfu New Area of Sichuan Province as an Example*; Chinese Society of Urban Planning: Beijing, China, 2016; p. 15.
45. Jin, H.; Liu, S.; Kang, J. Gender differences in thermal comfort on pedestrian streets in cold and transitional seasons in severe cold regions in China. *Build. Environ.* **2020**, *168*, 106488. [[CrossRef](#)]